Author Manuscript

Author Manuscript

Author Manuscript

Author Manuscript

HHS Public Access

Author manuscript

Nature. Author manuscript; available in PMC 2015 June 18.

Published in final edited form as:

Nature. 2014 December 18; 516(7531): 414–417. doi:10.1038/nature13818.

Mitochondrial UPR-regulated innate immunity provides resistance to pathogen infection

Mark W. Pellegrino[1], **Amrita M. Nargund**[1], **Natalia V. Kirienko**[3,4], **Reba Gillis**[1], **Christopher J. Fiorese**[2], and **Cole M. Haynes**[1,2,*]

[1]Cell Biology Program, Memorial Sloan Kettering Cancer Center, New York, NY 10065, USA

[2]BCMB Allied Program, Weill Cornell Medical College, 1300 York Avenue, New York, NY, USA

[3]Department of Molecular Biology, Massachusetts General Hospital, Boston, MA 02114, USA

[4]Department of Genetics, Harvard Medical School, Boston, MA, 02115, USA

Abstract

Metazoans identify and eliminate bacterial pathogens in microbe-rich environments such as the intestinal lumen, however the mechanisms are unclear. Potentially, host cells employ intracellular surveillance or stress response programs to detect pathogens that target monitored cellular activities to initiate innate immune responses[1–3]. Mitochondrial function is evaluated by monitoring mitochondrial protein import efficiency of the transcription factor ATFS-1, which mediates the mitochondrial unfolded protein response (UPR^{mt}). During mitochondrial stress, import is impaired[4] allowing ATFS-1 to traffic to the nucleus where it mediates a transcriptional response to re-establish mitochondrial homeostasis[5]. Here, we examined the role of ATFS-1 during pathogen exposure because in addition to mitochondrial protective genes, ATFS-1 induced innate immune genes during mitochondrial stress that included a secreted lysozyme and anti-microbial peptides. Exposure to the pathogen *Pseudomonas aeruginosa* caused mitochondrial dysfunction and activation of the UPR^{mt}. Animals lacking *atfs-1* were susceptible to *P. aeruginosa*, while hyper-activation of ATFS-1 and the UPR^{mt} improved clearance of *P. aeruginosa* from the intestine and prolonged *C. elegans* survival largely independent of known innate immune pathways[6,7]. We propose that ATFS-1 import efficiency and the UPR^{mt} is a means to detect pathogens that target mitochondria and initiate a protective innate immune response.

Animals harbor bacteria that are essential for normal physiology[8], however they must distinguish between commensal and pathogenic microbes to maintain homeostasis. Pathogenic bacteria can be recognized directly or by damage inflicted by the pathogen[9] leading to activation of innate immunity responses that limit pathogen growth. Recently, it has been demonstrated that perturbations to protein synthesis, proteolysis, or mitochondrial

Users may view, print, copy, and download text and data-mine the content in such documents, for the purposes of academic research, subject always to the full Conditions of use:http://www.nature.com/authors/editorial_policies/license.html#terms

*Correspondence: haynesc@mskcc.org.

AUTHOR CONTRIBUTIONS

MWP, AMN, NVK, RG and CJF performed experiments. MWP and CMH conceived of and planned the experiments and wrote the paper.

Author Manuscript Author Manuscript Author Manuscript Author Manuscript

activity are sufficient to activate innate immune responses suggesting the elegant hypothesis that host cells utilize intracellular stress responses to initiate innate immunity programs when pathogens perturb monitored cellular processes[1–3].

Cells respond to mitochondrial dysfunction by activating the UPR^{mt}, which is regulated by the transcription factor ATFS-1. In healthy cells, ATFS-1 is efficiently imported into mitochondria and degraded. However, during mitochondrial stress, import efficiency is reduced[4,5], allowing a small percentage of ATFS-1 to accumulate in the cytosol[5]. Because ATFS-1 has a nuclear localization sequence (NLS), it then traffics to the nucleus where it activates a protective transcriptional response (Fig. 1a). Our expression profiling studies indicated that ATFS-1 induces genes that promote mitochondrial protein folding, ROS detoxification and mitochondrial protein import, suggesting the UPR^{mt} stabilizes the mitochondrial protein folding environment to promote organelle homeostasis[5].

Intriguingly, a number of transcripts induced during mitochondrial stress caused by inhibition of the mitochondrial protease SPG-7 encode innate immunity proteins[5] (Extended Data Table 1), some of which were also found to be induced following exposure to the pathogen *P. aeruginosa*[10] (Fig. 1b and Extended Data Table 2). The antimicrobial peptide *abf-2* and the secreted lysozyme *lys-2*, both of which are required for resistance to pathogen infection[11,12], were induced during mitochondrial stress (Fig. 1c–d), as were two C-type lectins, which are involved in pathogen recognition[13] (Fig. 1e–f). Of note, mitochondrial-specific stress also caused induction of antimicrobial peptides[14] in mammalian cells (Fig. 1g–j), suggesting the response is conserved. In *C. elegans*, induction of innate immune genes by *spg-7*(RNAi) required ATFS-1 (Fig. 1c–f). Thus, in addition to inducing mitochondrial-protective genes, ATFS-1 also transcriptionally up-regulated innate immune genes during mitochondrial stress. Therefore, we hypothesized that ATFS-1 and the UPR^{mt} are involved in regulating innate immunity during exposure to pathogens that perturb mitochondrial function.

P. aeruginosa produces virulence factors that target many cellular functions including the mitochondrial toxins cyanide and pyocyanin[15,16]. *P. aeruginosa* also produces exotoxin A, which impairs protein synthesis and leads to the induction of the innate immune gene *irg-1* via the transcription factor ZIP-2[2,3,17]. Mitochondrial stress also caused *irg-1$_{pr}$::gfp* induction, which was blocked in *atfs-1(tm4919)* and partially so in *zip-2(tm4248)* worms (Fig. 1k), suggesting that multiple transcription factors and stressors influence innate immune gene expression. Additionally, *zip-2* mRNA was induced during mitochondrial stress, which also required *atfs-1* (Fig. 1l). Of note, *F35E12.5*, which is induced by the MAP kinase PMK-1 and the transcription factor ATF-7 during *P. aeruginosa* exposure[10,18], was not induced during mitochondrial stress (Extended Data Fig. 1a). Thus, ATFS-1 regulates a subset of innate immune genes during mitochondrial stress in addition to its cytoprotective role in promoting mitochondrial homeostasis.

We next examined if *P. aeruginosa* exposure caused mitochondrial stress capable of activating the UPR^{mt}. Slow-killing conditions were used in which the pathogen accumulates in the intestine leading to infection[19]. Interestingly, *P. aeruginosa* exposure caused intestinal cell mitochondria to elongate similar to *spg-7*(RNAi) (Fig. 2a), consistent with the pathogen

Author Manuscript Author Manuscript Author Manuscript Author Manuscript

causing mitochondria stress, and mitochondrial fusion providing protection[20]. Additionally, exposure to *P. aeruginosa* caused dramatic developmental delays in combination with mild mitochondrial stresses such as ethidium bromide[5], paraquat[5], or the *clk-1(qm30)* allele[21] (Fig. 2b), consistent with the pathogen causing modest mitochondrial stress. Importantly, *P. aeruginosa* exposure caused increased mitochondrial chaperone reporter (*hsp-6* and *hsp-60$_{pr}$::gfp*) activation in the intestine that required *atfs-1* (Fig. 2c and Extended Data Fig. 1b), which correlated with increased nuclear accumulation of ATFS-1::GFP and required the NLS in ATFS-1 (Fig. 2d and Extended Data Fig. 1c, d). Exposure to *P. aeruginosa* liquid-killing conditions, which requires pathogen expressed iron chelating siderophores[22], also induced mitochondrial chaperone genes, suggesting multiple *P. aeruginosa* virulence factors can activate the UPR^{mt} (Extended Data Fig. 2a, b). Interestingly, both synthetic growth arrest and UPR^{mt} activation by *P. aeruginosa* required the global virulence activator gene *gacA*[23] (Fig. 2b, c). Furthermore, exposure to *P. aeruginosa* strains lacking individual siderophore, pyocyanin or cyanide toxin genes resulted in less UPR^{mt} activation than wild-type *P. aeruginosa* (Extended Data Fig. 2d, e), suggesting that multiple pathogen toxins target mitochondrial function resulting in UPR^{mt} activation. However, UPR^{mt} activation may also be due to indirect damage associated with activation of a separate immune response[24].

We examined the role of ATFS-1 in the induction of innate immune genes during *P. aeruginosa* exposure rather than specifically during mitochondrial stress. Similarly, *abf-2*, *lys-2*, *clec-4* and *clec-65* were induced upon *P. aeruginosa* exposure, which also required *atfs-1* (Fig. 2e–h). And similar to the mitochondrial chaperones, both *lys-2$_{pr}$::gfp* and *irg-1$_{pr}$::gfp* were induced in the intestine upon *P. aeruginosa* exposure (Fig. 2i and Extended Data Fig 3). Interestingly, increased *irg-1$_{pr}$::gfp* expression was impaired in both *atfs-1(tm4919)* and *zip-2(tm4248)* mutants (Fig. 2i). Furthermore, *zip-2* transcript induction on *P. aeruginosa*[17] was also partially impaired in *atfs-1* mutant worms, suggesting *atfs-1* can function upstream of *zip-2* (Extended Data Fig. 4a).

Consistent with a role for ATFS-1 in inducing innate immune and mitochondrial protective genes[5], the survival of worms raised on *atfs-1*(RNAi) was significantly reduced when exposed to *P. aeruginosa*, but not *E. coli* (Fig. 3a–b). *atfs-1*(RNAi) treated worms were also susceptible to *P. aeruginosa* liquid-killing (Extended Data Fig. 2c), supporting a role for ATFS-1 in activating a protective transcriptional response to pathogen exposure. Of note, RNAi was used to reduce *atfs-1* activity for the survival studies rather than *atfs-1(tm4919)* because of germline defects that complicate the analysis (Extended Data Fig. 4b, c).

We next examined if UPR^{mt} activation is sufficient to protect against *P. aeruginosa*. The UPR^{mt} was induced by allowing worms to develop on *spg-7*(RNAi) for two days[5] prior to pathogen exposure. UPR^{mt} pre-activation dramatically reduced the intestinal accumulation of *P. aeruginosa* expressing GFP (*P. aeruginosa*-GFP[19] (Fig. 3c, d)). Importantly, *P. aeruginosa*-GFP accumulated in the intestine of *atfs-1(tm4919)* worms following *spg-7*(RNAi) treatment indicating that UPR^{mt} activation promotes pathogen clearance. In addition to adapting transcription, worms are also able to avoid *P. aeruginosa*, which was unaffected by *atfs-1(tm4919)* or pretreatment with *spg-7*(RNAi) (Extended Data Fig. 5a–e). Consistent with increased pathogen clearance via anti-microbial gene induction, UPR^{mt} pre-

Author Manuscript Author Manuscript Author Manuscript Author Manuscript

activation prolonged the survival of animals challenged with *P. aeruginosa*, which required *atfs-1* (Fig. 3e) and was independent of germline defects or feeding behavior (Extended Data Fig. 5f–g).

Because mitochondrial stress can activate multiple stress response pathways in addition to the UPR^{mt} [25,26], we examined an *atfs-1* gain-of-function mutant, which constitutively activates the UPR^{mt} independent of mitochondrial dysfunction. *atfs-1(et18)* worms express ATFS-1 with an amino acid substitution in the mitochondria targeting sequence that reduces mitochondrial import efficiency causing constitutive UPR^{mt} activation[27] and innate immune gene induction (Extended Data Fig. 6a–e). Impressively, *atfs-1(et18)* worms accumulated less *P. aeruginosa*-GFP in the intestine (Fig. 3f, g) and survived longer than wild-type worms (Fig. 3h) indicating that UPR^{mt} activation is sufficient to provide resistance to *P. aeruginosa*. Importantly, *atfs-1*(RNAi) and *lys-2*(RNAi) reduced *atfs-1(et18)* worm survival (Fig. 3h and Extended Data Fig. 6f), suggesting that ATFS-1-mediated innate immune gene induction provides resistance to *P. aeruginosa*.

Inhibition of additional cellular activities including translation (*eft-2*), mRNA splicing (*T08A11.2*), calcium transport (*sca-1*) and the pentose phosphate pathway (*T25B9.9*) also induce innate immune gene expression[1–3] but do not induce the UPR^{mt} (Extended Data Fig. 7a, b). Thus, we examined if other stress-activated innate immune responses are also protective against *P. aeruginosa*. Knockdown of *eft-2*, *T25B9.9*, *sca-1* or *T08A11.2* did not increase survival on *P. aeruginosa* (Extended Data Fig. 7c) however, *sca-1*(RNAi) and *T08A11.2*(RNAi) decreased lifespan on *E. coli*, indicating a reduction in general fitness (Extended Data Fig. 7d). In contrast, knockdown of the mitochondrial ATP synthase subunit *atp-2*, which activates mitochondrial protective and innate immune gene expression (Extended Data Fig. 7a, b), prolonged survival during *P. aeruginosa* exposure (Extended Data Fig. 7c). Our data suggest the UPR^{mt} provides protection from *P. aeruginosa* by coupling mitochondrial-protective and antimicrobial gene expression.

Lastly, we determined if ATFS-1 and the UPR^{mt} interacted with established *C. elegans* innate immune pathways, which include a MAP kinase pathway mediated by NSY-1/SEK-1/PMK-1[6,7,10], the MLK-1/MEK-1/KGB-1 c-Jun kinase pathway[7,28], as well as that mediated by ZIP-2[17]. Interestingly, pre-activation of the UPR^{mt} enhanced the survival of the *pmk-1* and *sek-1* mutants (Fig. 4a, b), as well as the *kgb-1* and *mlk-1* mutants (Fig. 4c, d). Of note, increased survival by *spg-7*(RNAi) was further enhanced in *kgb-1(km21)* worms, consistent with *kgb-1* being a negative regulator of the UPR^{mt} [29] (Extended Data Fig. 7e). Alternatively, *zip-2(tm4248)* modestly reduced the enhanced resistance conferred by *spg-7*(RNAi) (Fig. 4e), consistent with *atfs-1* functioning in the same pathway as *zip-2* during mitochondrial stress. In sum, our data suggest that the UPR^{mt} can function independent of the MAP and c-Jun kinase-regulated innate immune pathways.

Our studies indicate that the UPR^{mt} is activated by and protects against *P. aeruginosa*, and thus support a mechanistic means[5] by which host cells can detect pathogens that target mitochondrial function (Fig. 4f), which is consistent with only a subset of bacterial species inducing the UPR^{mt} [30]. Because ATFS-1 responds directly to mitochondrial dysfunction and induces a transcriptional response that is both mitochondrial protective[5] and antimicrobial,

Author Manuscript Author Manuscript Author Manuscript Author Manuscript

the UPR^{mt} is a uniquely comprised pathway to mitigate mitochondrial damage stemming from genetic defects or pathogen exposure (Fig. 4f).

METHODS

Worm and bacterial strains

The *atfs-1(tm4919)* mutant strain was a gift from the National BioResource Project and backcrossed to wild-type N2 twice. Worm strains were provided by the Caenorhabditis Genetics Center unless otherwise noted. Hermaphrodite worms were raised on the OP50 strain of *E. coli* unless they were treated with RNAi, in which the HT115 *E. coli* strain expressing the described RNAi plasmid was used[31,32]. Where indicated, worms were exposed to the pathogenic strain of *P. aeruginosa*, PA14.

Cell culture

Expression of dominant-negative AFG3L2 was induced in stable HEK293 cells by the addition of 1μg/ml tetracycline[33] and the cells were harvested 48 hours later. The ΔOTC expression plasmid[34] was transfected into Hela cells via Lipofectamine and the cells were harvested after 72 hours.

C. elegans slow-killing assay

Slow-killing experiments were performed as previously described[35,36] with minor modifications. *E. coli* or *P. aeruginosa* overnight cultures were used to seed slow-killing nematode growth medium (NGM) agar plates (with 0.35% peptone). Plates were allowed to dry overnight at room temperature, incubated at 37°C for 24 hours and allowed to equilibrate at room temperature. Synchronized L1 worms were allowed to develop on *E. coli* until the L4 stage and then transferred to *P. aeruginosa* slow-killing plates and incubated at 25°C. RNAi was performed as described previously[37]. For *atfs-1*(RNAi) (Fig. 3a–b), *eri-1(mg366)* (enhanced RNAi) worms[38] were raised on control or *atfs-1*(RNAi) bacteria at 16°C until the L4 stage. All animals were transferred to fresh *P. aeruginosa* slow-killing plates in a randomized fashion. Animals were counted at the described times and were scored as dead if they failed to respond when touched. Fifty worms were used per experiment and those that had crawled off the plate or exploded at the vulva were censored. All data related to the survival analysis is presented in Extended Data Table 3. Each experiment was performed in triplicate and the log rank (Mantel-Cox) statistical test was used to evaluate *p* values.

Intestinal mitochondrial morphology was visualized using *ges-1$_{pr}$::gfp^{mt}* worms[39]. The worms were synchronized by bleaching and allowed to hatch on plates containing *P. aeruginosa* and raised for 48 hours at 25°C. Visualization of *hsp-6$_{pr}$::gfp*, *hsp-60$_{pr}$::gfp* and *atfs-1$_{pr}$::atfs-1::gfp* was performed essentially as described[36,37]. *P. aeruginosa* was grown at 16°C for 24 hours and seeded onto slow-killing plates. Plates were incubated overnight at room temperature. Synchronized L1s were transferred to *P. aeruginosa* plates and incubated at 20°C for 24 hours before imaging.

Author Manuscript Author Manuscript Author Manuscript Author Manuscript

To examine growth rates, eggs were allowed to hatch on plates containing *P. aeruginosa* and raised for 3 days at 25°C. 30 μg/ml ethidium bromide or 0.2 mM paraquat was added to *E. coli* or *P. aeruginosa* slow-killing plates. For *clk-1(qm30)* growth rates, worms were raised for 4 days at 25°C.

Statistics

All experiments were performed three times yielding similar results and comprised of biological replicates. The sample size and statistical tests were chosen based on previous studies with similar methodologies and the data met the assumptions for each statistical test performed. No statistical methods were used in deciding sample sizes, nor were any blinded experiment performed. For all figures, the mean ± standard deviation (SD) is represented unless otherwise noted.

C. elegans liquid-killing assay

glp-4(bn2) worms were raised at 25°C to sterilize them while being fed *atfs-1*(RNAi). At the L4-early adult stage, the described worms were exposed to *P. aeruginosa* under conditions used for the liquid-killing assay[40].

RNA isolation and quantitative real time PCR (qRT-PCR)

Total RNA was obtained using the RNA STAT reagent (Tel-Test Inc.) and used for cDNA synthesis via the iScript™ cDNA Synthesis Kit (Bio-Rad Laboratories). qRT-PCR was performed using Thermo-Scientific™; SyBr Green Maxima Mix. For Figures 1c–f and 1l, worms were hatched onto RNAi-expressing plates and harvested after 48 hours. For Figures 2e–h, synchronized L4 worms were fed on *E. coli* or *P. aeruginosa* for 8 hours using the slow-killing method prior to harvesting. For Extended Data Figures 2a–b, synchronized *glp-4(bn2)* L4 worms were raised in liquid culture using *E. coli* or *P. aeruginosa* for 16 hours. All values were normalized to wild-type worms grown on control bacteria for RNAi experiments (Fig. 1c–f, l) or wild-type worms grown on *E. coli* for *P. aeruginosa* experiments (Fig. 2e–h). *act-3* and *snb-1* mRNA were used as controls for slow-killing and liquid-killing experiments, respectively. HPRT mRNA was used as a control for dominant-negative AFG3L2 and ΔOTC experiments.

Primer sequences used for qRT-PCR: *act-3*: forward ATCCGTAAGGACTTGTACGCCAAC and reverse CGATGATCTTGATCTTCATGGTTC, *abf-2*: forward CGTGGCTGCCGACATCGACTT and reverse ATGCACAACCCCTGAGCCGC, *lys-2*: forward ATCGACTCGAACCAAGCTGCG and reverse TCGACAGCATTTCCCATTGAAGCGT, *clec-4*: forward GAGCGACACTGGTGACTGTG and reverse CCATCCAGAATAGGTTGGCG, *clec-65*: forward CCCGGTGGTGACTGTGAATA and reverse AGCTCATATTGTCGCTGGCA, *zip-2*: forward TCGACGAGCAAACGACCTAC and reverse CTTGTGGCGTGCTCATGTT, *hsp-60*: forward AGGGATTCGAGAGCATTCGTCAAG and reverse TGTGGCGACTTGAGCGATCTCTTC, *hsp-6*: forward GAAGATACGAAGACCCAGAGGTTC and reverse CAACCTGAGATGGGGAATACACT, *snb-1*: forward CCGGATAAGACCATCTTGACG

Author Manuscript Author Manuscript Author Manuscript Author Manuscript

and reverse GACGACTTCATCAACCTGAGC, hBD-2: forward GCCTCTTCCAGGTGTTTTTG and reverse GAGACCACAGGTGCCAATTT, hBD-4: forward ATGTGGTTATGGGACTGCCC and reverse AGCATGCATAGGTGTTGGGA, HD-5: forward TCCTTGCTGCCATTCTCCTG and reverse ACTGCTTCTGGGTTGTAGCC, LL-37: forward GCTGGGTGATTTCTTCCGGA and reverse CCTGGGTACAAGATTCCGCA, HPRT: forward CTTTGCTGACCTGCTGGATT and reverse TCCCCTGTTGACTGGTCATT.

P. aeruginosa intestinal accumulation assay

To examine bacterial accumulation in the worm intestine, wild-type or *atfs-1(tm4919)* worms were synchronized and raised on control or *spg-7*(RNAi) plates for 48 hours. Overnight cultures of *P. aeruginosa* expressing GFP (*P. aeruginosa*-GFP) were seeded onto slow-killing NGM plates, allowed to dry overnight at room temperature and then incubated at 37°C for 24 hours. To exclude pathogen avoidance as a means of decreased intestinal colonization, where indicated *P. aeruginosa*-GFP was also spread across the entire surface of the slow-killing plate (Extended Data Fig. 5d, e). Worms at the L4 stage were transferred to *P. aeruginosa*-GFP plates and allowed to feed for 24–48 hours prior to examination. The extent of bacterial accumulation was scored as either “none/mild”, “moderate” or “strong” as indicated (Extended Data Fig. 5c).

Plasmid construction

The *hsp-16*$_{pr}$*::atfs-1*^{FL} and *hsp-16*$_{pr}$*::atfs-1*$^{\Delta NLS}$ plasmids were described previously[37]. To construct the *lys-2*$_{pr}$*::gfp* plasmid, a 803 base pair fragment of the *lys-2* promoter sequence upstream of the start codon was amplified using PCR and cloned into the *HindIII* and *PstI* sites of pPD95.75. *lys-2*$_{pr}$*::gfp* was microinjected into wild-type worms at a concentration of 20 ng/μl along with *myo-3*$_{pr}$::mCherry at a concentration of 60 ng/μl.

P. aeruginosa avoidance assay

Synchronized L1 wild-type and *atfs-1(tm4919)* worms were allowed to develop on control or *spg-7*(RNAi) plates to the L4 stage and then transferred to *E. coli* or *P. aeruginosa* slow-killing plates for 17 hours when the worms were scored. The extent of avoidance was expressed as the percent of animals off of the bacterial lawn over the total the number of animals on the plate (Extended Data Fig. 5a, b).

Microscopy

C. elegans were imaged using a Zeiss AxioCam MRm mounted on a Zeiss Imager.Z2 microscope. Exposure times were the same in each experiment.

Author Manuscript Author Manuscript Author Manuscript Author Manuscript

EXTENDED DATA

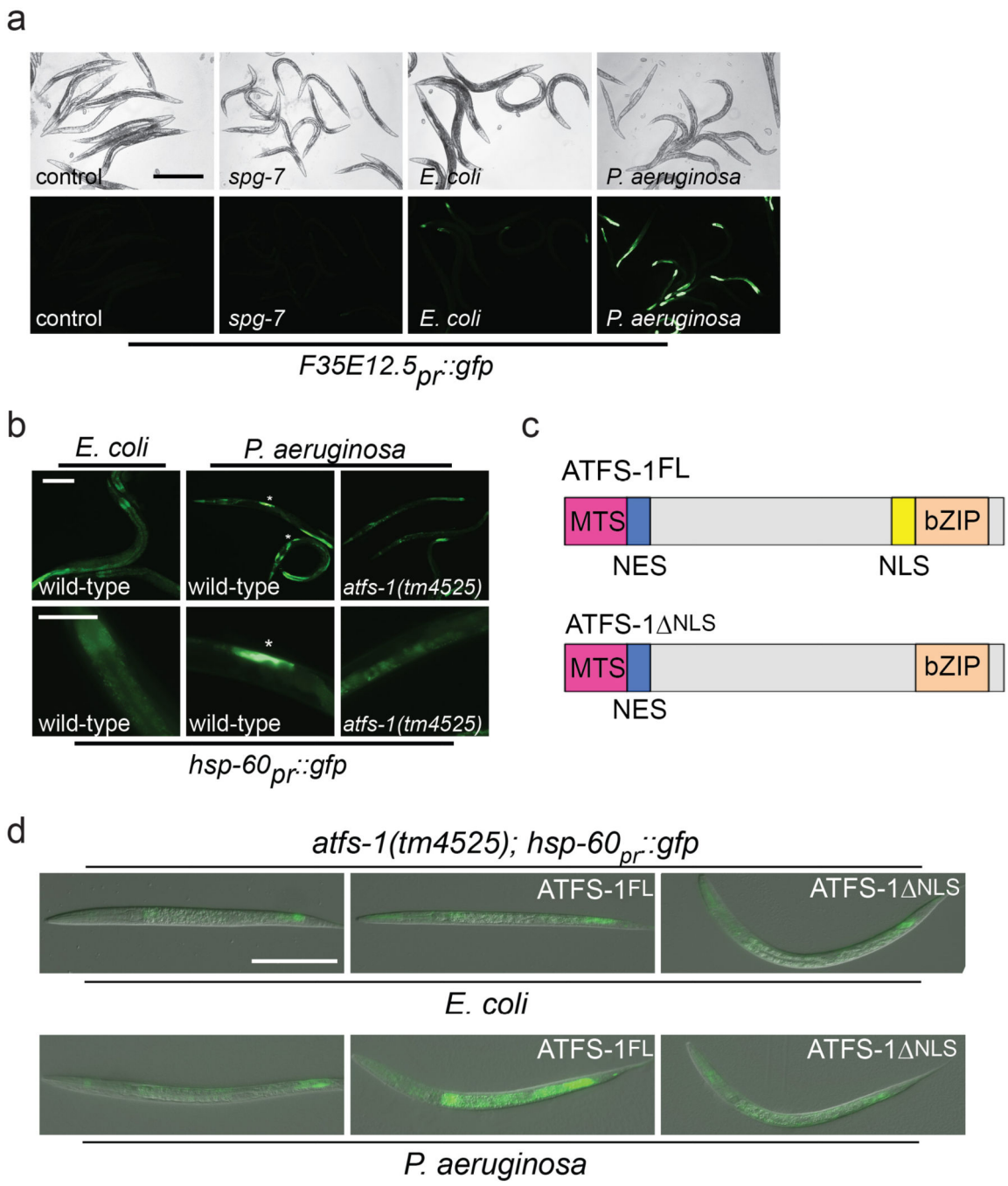

Extended Data Figure 1. Nuclear accumulation of ATFS-1 is required for UPR^{mt} activation during *P. aeruginosa* exposure

a, Representative photomicrographs of *F35E12.5*$_{pr}$*::gfp* transgenic worms raised on control or *spg-7*(RNAi). No detectable increase in expression was observed following *spg-7*(RNAi) treatment. In contrast, strong expression of *F35E12.5*$_{pr}$*::gfp* was observed following exposure to *P. aeruginosa* compared to *E. coli* controls. Scale bar, 0.5 mm.

Author Manuscript Author Manuscript Author Manuscript Author Manuscript

b, Wild-type or *atfs-1(tm4525);hsp-60$_{pr}$::gfp* worms on *E. coli* or *P. aeruginosa*. Lower panels are magnified views of the intestine showing enhanced expression of *hsp-60$_{pr}$::gfp* (asterisks). Scale bars, 0.05 mm.

c, Diagrams of wild-type ATFS-1 (ATFS-1^{FL}) and ATFS-1 with a mutated nuclear localization signal (ATFS-1$^{\Delta NLS}$).

d, Photomicrographs of *atfs-1(tm4525);hsp-60$_{pr}$::gfp* worms expressing ATFS-1^{FL} or ATFS-1$^{\Delta NLS}$ via the *hsp-16* promoter exposed to *E. coli* or *P. aeruginosa*. Scale bar, 0.1 mm.

Author Manuscript Author Manuscript Author Manuscript Author Manuscript

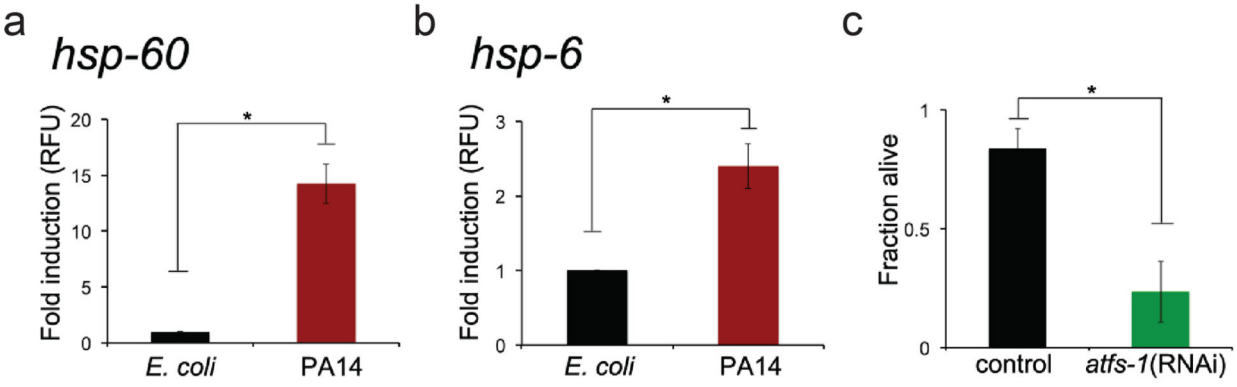

d

GENE NAME	FUNCTION
pvdA	Iron chelation
pvdD	Iron chelation
pvdF	Iron chelation
phzM	Pyocyanin production
hcnB	Hydrogen cyanide production
hcnC	Hydrogen cyanide production

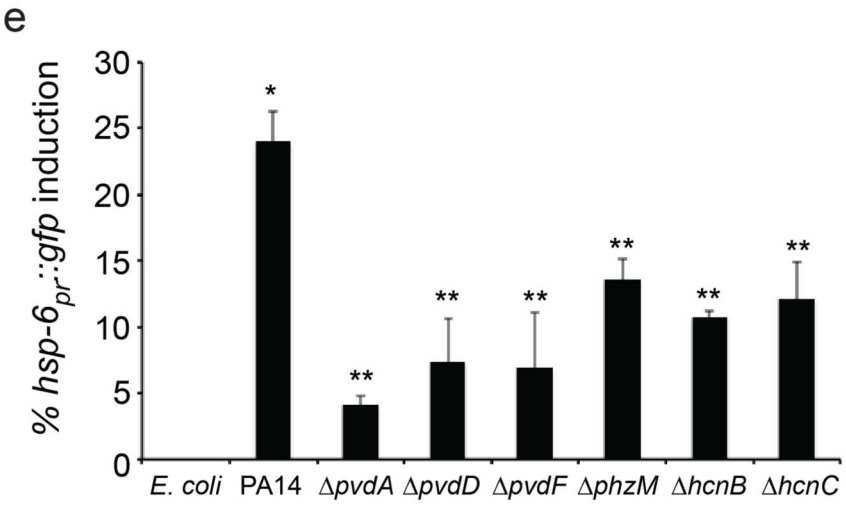

Extended Data Figure 2. Multiple *P. aeruginosa* virulence genes contribute to UPR^{mt} activation

a–b, Expression of *hsp-60* and *hsp-6* mRNA for *glp-4(bn2)* worms exposed to *E. coli* or *P. aeruginosa* liquid-killing using qRT-PCR (N=3, ± SD). Fold inductions are normalized to wild-type *E. coli* test group, * $p<0.05$ (Student t-test).

c, Quantitation of survival for *glp-4(bn2)* worms raised on control or *atfs-1*(RNAi) and exposed to *P. aeruginosa* liquid-killing, *$p<0.0001$ (Student t-test).

d, List of *P. aeruginosa* toxin mutants.

Author Manuscript Author Manuscript Author Manuscript Author Manuscript

e, Quantitation of the proportion of worms showing increased *hsp-6*$_{pr}$*::gfp* expression in the intestine under slow-killing conditions. Exposure to *P. aeruginosa* caused *hsp-6*$_{pr}$*::gfp* induction (N=3, ± SE), *p<0.05 (Student t-test). However, exposure to *P. aeruginosa* with mutations in the *pvdA, pvdD, pvdF, phzM, hcnB,* or *hcnC* toxin genes resulted in relatively less UPR^{mt} activation (N=3, ± SE), **p<0.05 (Student t-test).

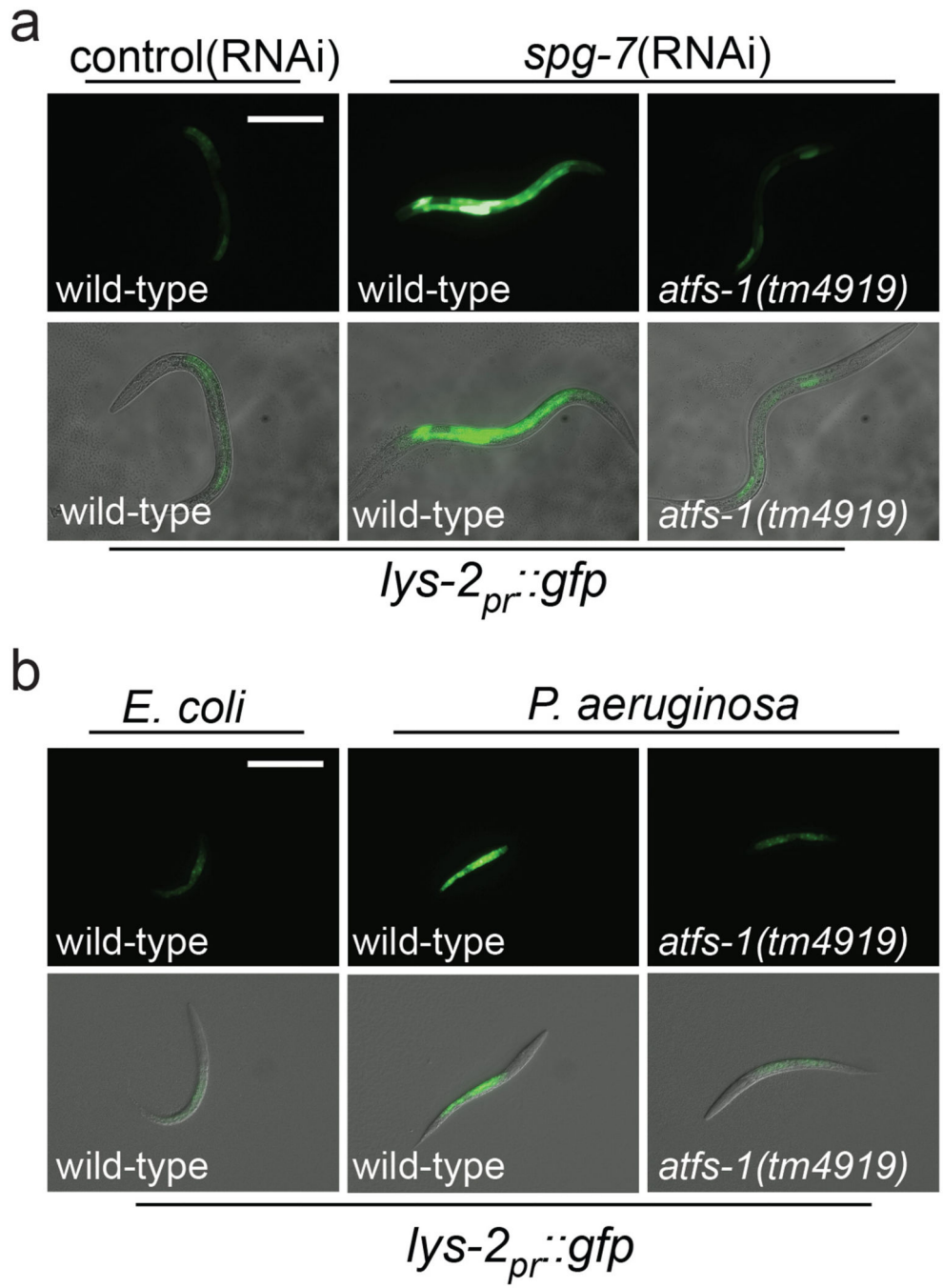

Extended Data Figure 3. Intestinal accumulation of *lys-2* during mitochondrial stress and *P. aeruginosa* exposure requires ATFS-1

Author Manuscript Author Manuscript Author Manuscript Author Manuscript

a, Representative photomicrographs of wild-type and *atfs-1(tm4919)* worms carrying the *lys-2*$_{pr}$::*gfp* transgene raised on control or *spg-7*(RNAi). Scale bar, 0.1 mm.
b, Representative photomicrographs of wild-type and *atfs-1(tm4919)* worms carrying the *lys-2*$_{pr}$::*gfp* transgene exposed to *E. coli* or *P. aeruginosa*. Scale bar, 0.1 mm.

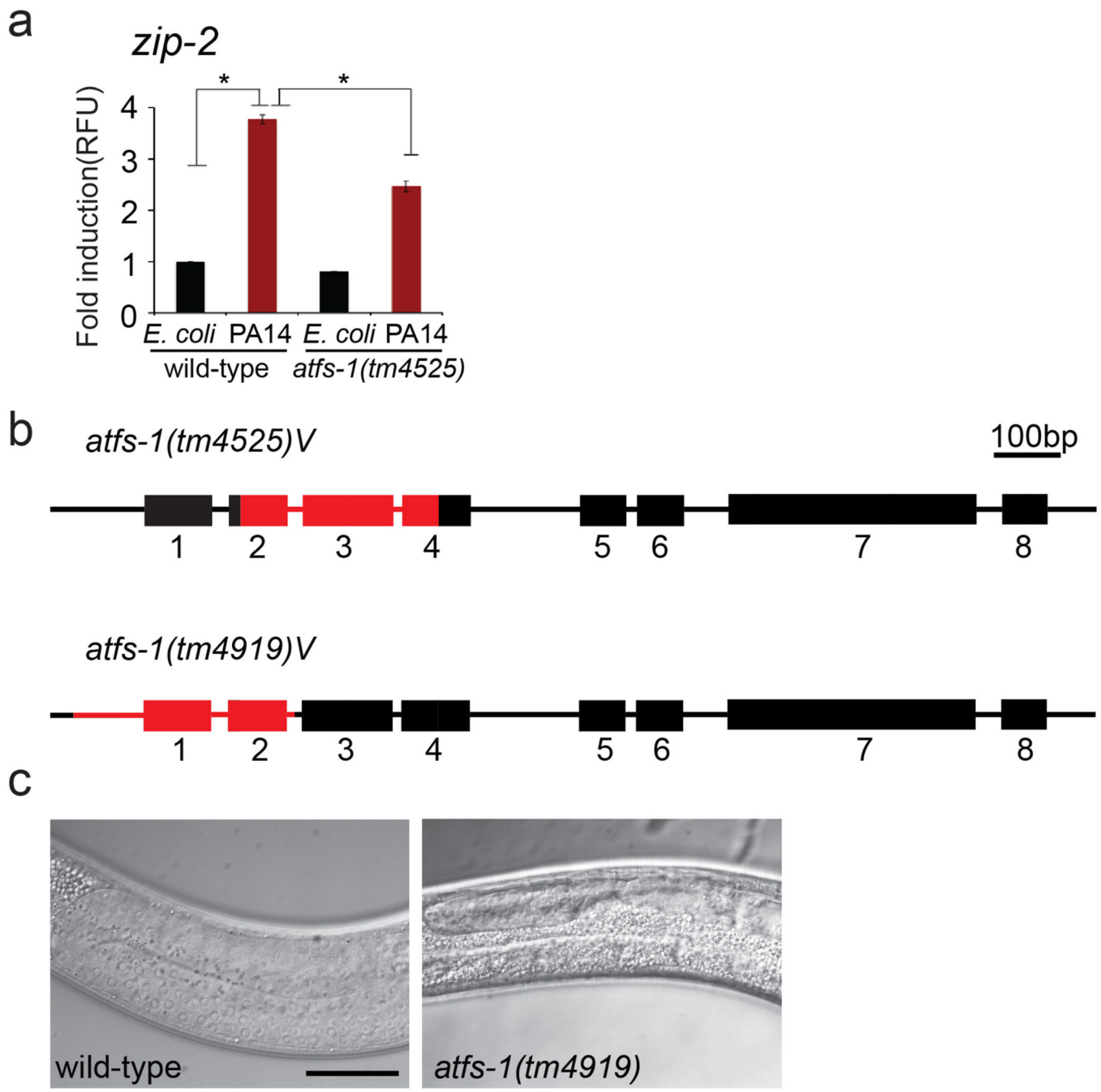

Extended Data Figure 4. ATFS-1 partially regulates *zip-2* expression during *P. aeruginosa* exposure

a, Expression levels of *zip-2* mRNA in wild-type or *atfs-1(tm4525)* worms raised on *E. coli* or *P. aeruginosa* using qRT-PCR (N=3, ± SD), * $p<0.05$ (Student's *t* test).

Author Manuscript Author Manuscript Author Manuscript Author Manuscript

b, Schematic diagram of the *atfs-1* genomic open reading frame showing positions of exons 1–8 (boxes) and locations of the *tm4525*[5] and *tm4919* deletions in red. The *tm4919* allele is a 334 base pair deletion beginning 107 base pairs upstream of the *atfs-1* start codon and ends within the second intron of the *atfs-1* genomic open reading frame.
c, Representative photomicrographs of a germline in wild-type and *atfs-1(tm4919)* worms. Scale bar, 0.02 mm.

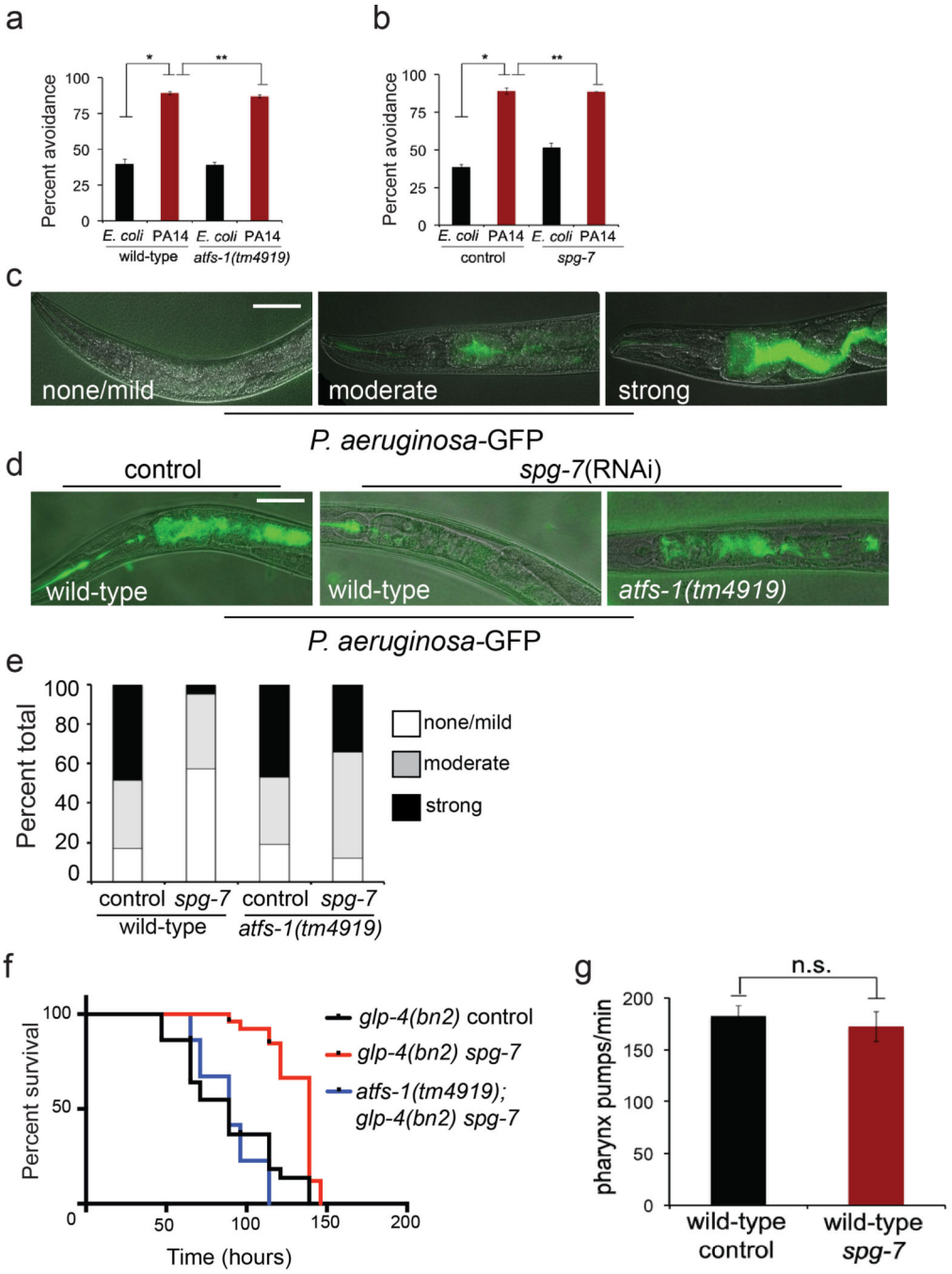

Extended Data Figure 5. ATFS-1 is not required for pathogen avoidance during *P. aeruginosa* exposure

Author Manuscript Author Manuscript Author Manuscript Author Manuscript

a, Quantitation of avoidance behavior for wild-type and *atfs-1(tm4919)* worms raised on *E. coli* or *P. aeruginosa* expressed as a percentage of the number of animals off the bacterial lawn relative to the total number worms (N=4, ± SD). **p*<0.0001, ***p*=0.1914 (Student t-test).

b, Quantitation of avoidance behavior for wild-type worms raised on control or *spg-7*(RNAi) and exposed to *E. coli* or *P. aeruginosa* expressed as a percentage of the number of animals off the bacterial lawn relative to the total number worms (N=3, ± SD). **p*<0.0001, ***p*=0.8706 (Student t-test).

c, Representative photomicrographs illustrating the scored level of infection for *P. aeruginosa* colonization assay using *P. aeruginosa*-GFP. Three categories of *P. aeruginosa*-GFP infection were used: none/mild, moderate and strong. Scale bar, 0.1 mm.

d, Representative photomicrographs of wild-type and *atfs-1(tm4919)* worms raised on *spg-7*(RNAi) and exposed to a lawn of *P. aeruginosa*-GFP that completely covered the surface of the slow-killing plate for 24 hours. Images are overlays of DIC and GFP. Scale bar, 0.1 mm.

e, Quantitation of *P. aeruginosa* intestinal colonization as shown in Extended Data Fig. 5d. White, grey and black bars denote no/mild infection, moderate infection and strong infection, respectively. Forty worms were analyzed per treatment.

f, Survival analysis of *glp-4(bn2)* and *atfs-1(tm4919); glp-4(bn2)* worms raised on control or *spg-7*(RNAi) and exposed to *P. aeruginosa*. Statistics for each survival analysis are presented in Extended Data Table 3.

g, Quantitation of pharyngeal pumping rate per minute for wild-type worms raised on control or *spg-7*(RNAi) (N=10, + SD). n.s., no significant difference (*p*=0.10; Student t-test).

Author Manuscript Author Manuscript Author Manuscript Author Manuscript

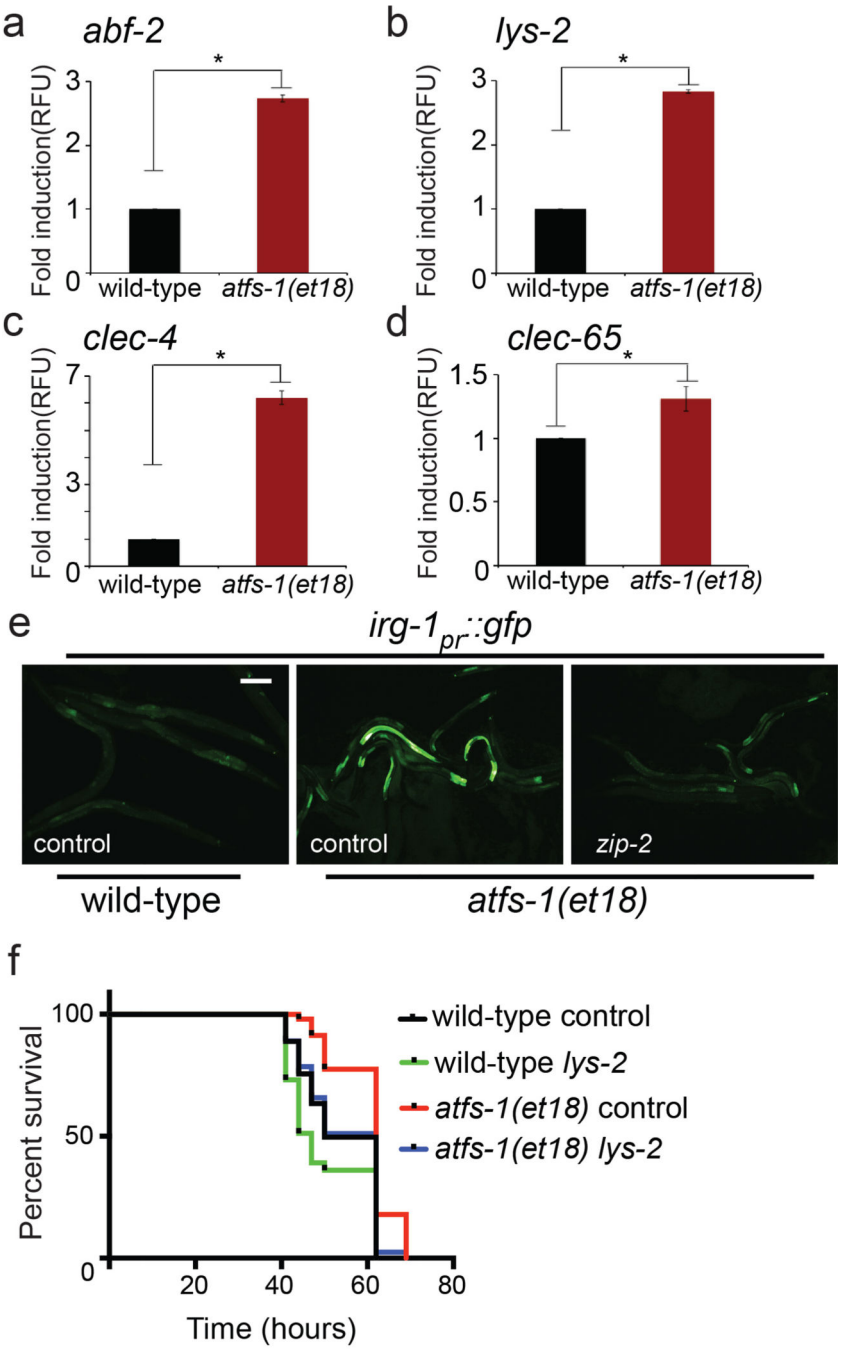

Extended Data Figure 6. *atfs-1(et18)* gain of function mutant worms induce innate immune gene expression in the absence of mitochondrial stress

a–d, Expression levels of *abf-2*, *lys-2*, *clec-4* and *clec-65* mRNA in wild-type or *atfs-1(et18)* worms using qRT-PCR (N=3, ± SD), * $p<0.05$ (Student's *t* test).

e, Representative photomicrographs of wild-type and *atfs-1(et18)* worms carrying the *irg-1*$_{pr}$*::gfp* transgene raised on control or *zip-2*(RNAi). Scale bar, 0.10 mm.

Author Manuscript Author Manuscript Author Manuscript Author Manuscript

f, Survival analysis of wild-type and *atfs-1(et18)* worms raised on control or *lys-2*(RNAi) and exposed to *P. aeruginosa*. Statistics for each survival analysis are presented in Extended Data Table 3.

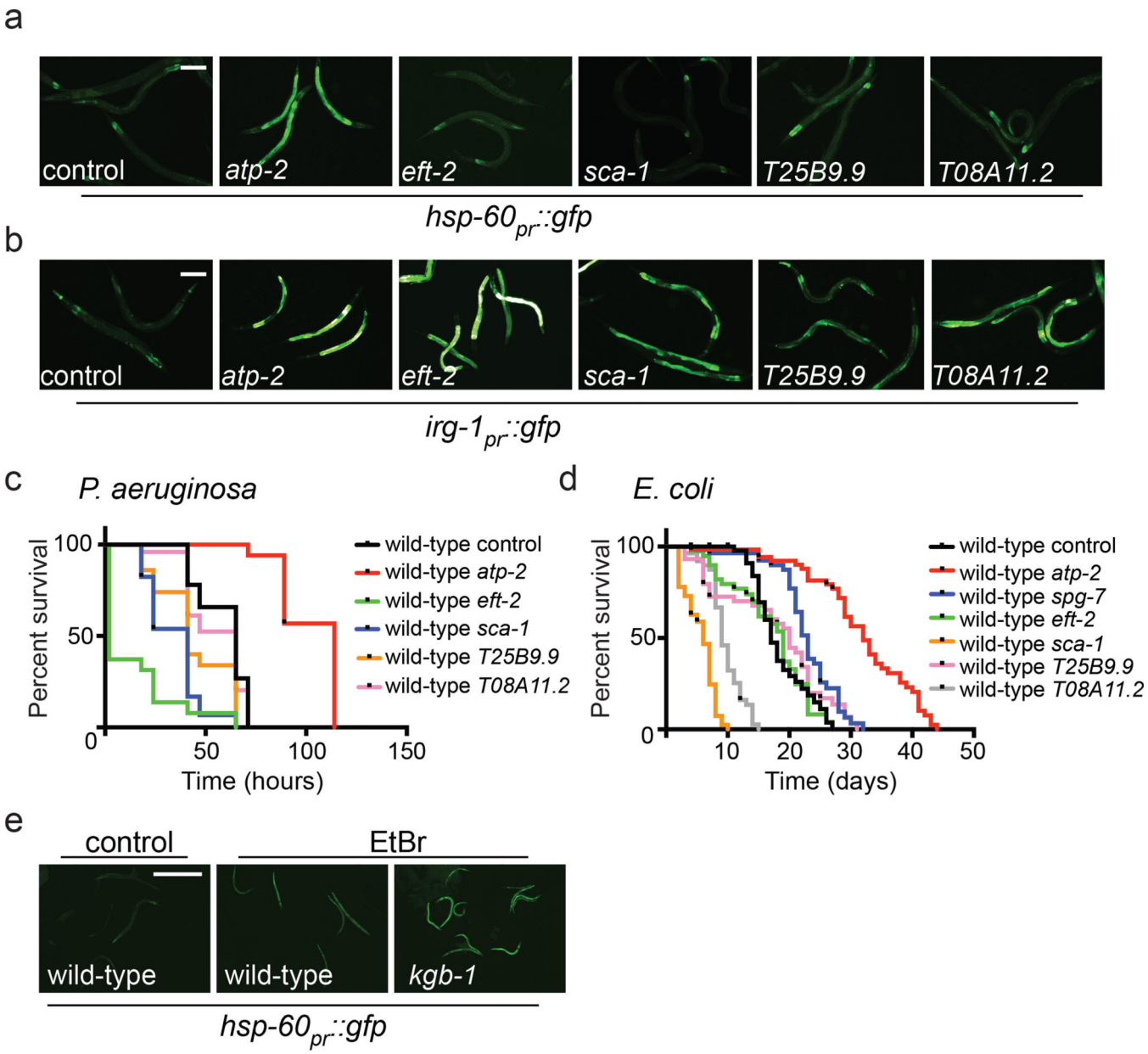

Extended Data Figure 7. Mitochondrial protective and innate immune gene induction contributes to ATFS-1-mediated resistance to *P. aeruginosa* infection

a, Representative photomicrographs of wild-type *hsp-60$_{pr}$::gfp* worms raised on control, *atp-2*(RNAi), *spg-7*(RNAi), *eft-2*(RNAi), *sca-1*(RNAi), *T25B9.9*(RNAi) or *T08A11.2*(RNAi). Scale bar is 0.1 mm.

b, Representative photomicrographs of wild-type *irg-1$_{pr}$::gfp* worms raised on control, *atp-2*(RNAi), *eft-2*(RNAi), *sca-1*(RNAi), *T25B9.9*(RNAi) or *T08A11.2*(RNAi). Scale bar is 0.1 mm.

Author Manuscript Author Manuscript Author Manuscript Author Manuscript

c, Survival analysis of wild-type worms raised on control, *atp-2*(RNAi), *eft-2*(RNAi), *sca-1*(RNAi), *T25B9.9*(RNAi) or *T08A11.2*(RNAi) and exposed to *P. aeruginosa*. Statistics for each survival analysis are presented in Extended Data Table 3.

d, Survival analysis of wild-type worms raised on control, *atp-2*(RNAi), *eft-2*(RNAi), *sca-1*(RNAi), *T25B9.9*(RNAi) or *T08A11.2*(RNAi) and exposed to *E. coli*. Statistics for each survival analysis are presented in Extended Data Table 3.

e, Representative photomicrographs of wild-type or *kgb-1(km21);hsp-60*$_{pr}$*::gfp* worms raised on *E. coli* plates with or without 30 μg/ml ethidium bromide suggesting the KGB-1 Jun kinase pathway negatively regulates the UPR^{mt} during mitochondrial stress[29]. Scale bar is 0.5 mm.

Extended Data Table 1

ATFS-1 dependent innate immune genes up-regulated when raised on *spg-7*(RNAi).

Sequence Name	Gene symbol	KOG title, protein domain or function	Fold Induction Wild-type *spg-7*(RNAi)/control	Fold Induction *atfs-1(tm4525)* *spg-7*(RNAi)/control
Antimicrobial peptides				
g6714550	*abf-2*	antimicrobial peptide	10.456	2.33072
R09B5.9	*cnc-4*	Caenorhabditis bacteriocin	4.58689	1.59881
Lysozyme				
Y22F5A.5	*lys-2*	N-acetylmuraminidase/lysozyme	4.81394	2.87725
C-type lectins				
F35C5.9	*clec-66*	Lectin C-type domain/CUB domain	3.60596	2.09418
F35C5.5	*clec-62*	Lectin C-type domain/CUB domain	3.81898	2.47423
F35C5.8	*clec-65*	Lectin C-type domain	4.366	2.25587
E03H4.10	*clec-17*	C-type lectin	21.9148	7.58123
C03H5.1	*clec-10*	C-type lectin	3.47056	1.82945
F31D4.4	*clec-264*	C-type lectin	1.87899	1.24332
T09F5.9	*clec-47*	C-type lectin	5.57165	−1.12101
Y38E10A.5	*clec-4*	C-type lectin	8.25168	3.66069
M02F4.7	*clec-265*	C-type lectin	8.40775	4.75704
F08H9.7	*clec-56*	C-type lectin	2.30962	1.32766
Galectin				
F38A5.3	*lec-11*	Galectin, galactose-binding lectin	2.29608	1.41767
Signalling				
F08B1.1	*vhp-1*	Dual specificity phosphatase	2.39868	1.59839

Author Manuscript Author Manuscript Author Manuscript Author Manuscript

Extended Data Table 2

ATFS-1 dependent UPRmt genes in common with genes induced following *P. aeruginosa* exposure.

Sequence name	Gene symbol	KOG title, protein domain or function	Fold Induction Wild-type *spg-7*(RNAi)/ control (Nargund et al., 2012	Fold Induction Wild-type PA14/ OP50 (Troemel et al. 2006 or this study*)
R08F11.3	*cyp-33C8*	Cytochrome P450 CYP2 subfamily	52.7502	4.1
T10B9.2	*cyp-13A5*	CYtochrome P450 family	35.6897	2.8
E03H4.10	*clec-17*	C-type lectin	21.9148	7.9
C54D10.1	*cdr-2*	glutathione S-transferase-like protein	15.2001	2.6
K01D12.11	*cdr-4*	cadmium responsive	11.9017	4
g6714550	*abf-2*	antimicrobial peptide	10.456	1.89*
F15B9.6			9.37816	2.7
K10D11.2			8.84434	3.1
M02F4.7	*clec-265*	C-type Lectin	8.40775	3.9
Y38E10A.5	*clec-4*	C-type Lectin	8.25168	11.1
C49G7.5			7.7102	21
C18A11.1			7.43593	3.1
F22H10.2			7.33184	4.4
C49G7.10			7.14237	9.7
C10C5.2			6.85214	5.9
Y58A7A.5			5.84559	12
R11G11.12	*nhr-210*	Nuclear Hormone Receptor family	5.76655	2.3
T12G3.1		contains ZZ-type Zn-finger	5.74038	3
ZK970.7			5.46349	3.9
R09B5.9	*cnc-4*	Caenorhabditis bacteriocin	4.58689	4.2
C49G7.7			4.41335	5.6
F35C5.8	*clec-65*	Lectin C-type domain	4.366	2.9
Y58A7A.3			4.34718	5.7
C34H4.2			4.34064	2.3
T16G1.5		Predicted small molecule kinase	4.25188	8.9
F01G10.3	*ech-9*	Hydroxyacyl-CoA dehydrogenase/enoylCoA hydratase	4.17949	5
T12G3.1		Uncharacterized conserved protein	4.09838	2.4
C50F4.1			4.07802	2.1
B0218.2	*faah-2*	amidase	3.8877	2.2
F19B2.5		Helicase-like transcription factor	3.81204	2.3
C50F4.1			3.78737	2.1
F35C5.9	*clec-66*	Lectin C-type domain/CUB domain	3.60596	6.2
M01G12.9			3.57904	3.2

Author Manuscript Author Manuscript Author Manuscript Author Manuscript

Sequence name	Gene symbol	KOG title, protein domain or function	Fold Induction Wild-type *spg-7*(RNAi)/ control (Nargund et al., 2012	Fold Induction Wild-type PA14/ OP50 (Troemel et al. 2006 or this study*)
K10G4.3			3.56853	2.2
C03H5.1	*clec-10*	C-type lectin	3.47056	2.3
C34C6.7			3.17263	2.6
Y22D7AR.9	*fbxa-74*	F-box A protein	3.10471	8.7
Y119D3B.20	*fbxa-92*	F-box A protein	3.06775	4.1
F55C12.7	*tag-234*		3.02488	3.5
Y17G7B.8			3.02481	2.2
C29F9.3			3.02333	2.6
C34D1.5	*zip-5*	bZip transcription factor	2.98077	2
Y58A7A.4			2.95958	2.2
T01D3.6		von Willebrand factor	2.91981	2.6
ZK418.7			2.55033	2.4
F49F1.6		Secreted surface protein	2.48376	17.6
K08D8.6			2.41167	3.6
C09F12.1	*cic-1*	claudin homolog	2.36493	2.3
T27F2.4		bZip transcription factor	2.35058	2.8
F38A5.3	*lec-11*	Galectin, galactose-binding lectin	2.29608	2.4
Y47H10A.5			2.24131	3.9
Y43C5A.3			2.06783	2.5
F23H12.3			1.77139	2
E02C12.8		Predicted small molecule kinase	1.7588	3.7
Y95B8A.6			1.67149	2.5
F11D11.3			1.55814	3.4
C50F4.9			1.54636	3.4
Y22F5A.5	*lys-2*	lysozyme	4.81394	10.6*

* this study

Extended Data Table 3

Statistics for survival analysis.

Strain comparison	*p* values	Number of worms	Figure
eri(mg366) control vs *eri-1(mg366) atfs-1*(RNAi)	0.0003	*eri(mg366)* control: 34/50, *eri-1(mg366) atfs-1*(RNAi): 39/50	3a
eri(mg366) control vs *eri-1(mg366) atfs-1*(RNAi)	0.6986	*eri(mg366)* control: 50/50, *eri-1(mg366) atfs-1*(RNAi): 47/50	3b
wild-type control vs wild-type *spg-7*(RNAi)	<0.0001	wild-type control: 37/50, wild-type spg-7(RNAi): 45/50	3e
wild-type *spg-7*(RNAi) vs *atfs-1(tm4919) spg-7*(RNAi)	<0.0001	wild-type *spg-7(RNAi):* 37/50, *atfs-1(tm4919) spg-7*(RNAi): 50/50	3e

Author Manuscript Author Manuscript Author Manuscript Author Manuscript

Strain comparison	*p* values	Number of worms	Figure
wild-type control vs *atfs-1(tm4919) spg-7*(RNAi)	0.1322	wild-type control: 37/50, *atfs-1(tm4919) spg-7*(RNAi): 50/50	3e
wild-type control vs *atfs-1(et18)* control	<0.0001	wild-type control: 41/50, *atfs-1(et18)* control: 30/50	3h
wild-type control vs wild-type *atfs-1*(RNAi)	0.039	wild-type control: 41/50, wild-type *atfs-1*(RNAi): 45/50	3h
atfs-1(et18) control vs *atfs-1(et18) atfs-1*(RNAi)	<0.0001	*atfs-1(et18)* control: 30/50, *atfs-1(et18): atfs-1*(RNAi): 37/50	3h
wild-type control vs *pmk-1(km25)* control	<0.0001	wild-type control: 33/50, *pmk-1(km25)* control: 42/50	4a
wild-type control vs wild-type *spg-7*(RNAi)	<0.0001	wild-type control: 33/50, wild-type *spg-7*(RNAi): 45/50	4a
pmk-1(km25) control vs *pmk-1(km25) spg-7*(RNAi)	<0.0001	*pmk-1(km25)* control: 42/50, *pmk-1(km25) spg-7*(RNAi): 23/50	4a
wild-type control vs *sek-1(km4)* control	<0.0001	wild-type control: 35/50, *sek-1(km4)* control: 35/50	4b
wild-type control vs wild-type spg-7(RNAi)	<0.0001	wild-type control: 35/50, wild-type *spg-7*(RNAi): 37/50	4b
sek-1(km4) control vs *sek-1(km4) spg-7*(RNAi)	<0.0001	*sek-1(km4)* control: 35/50, *sek-1(km4) spg-7*(RNAi): 39/50	4b
wild-type control vs *kgb-1(km21)* control	<0.0001	wild-type control: 29/50, *kgb-1(km21)* control: 38/50	4c
wild-type control vs wild-type *spg-7*(RNAi)	<0.0001	wild-type control: 29/50, wild-type *spg-7*(RNAi): 27/50	4c
kgb-1(km21) control vs *kgb-1(km21) spg-7*(RNAi)	<0.0001	*kgb-1(km21)* control: 38/50, *kgb-1(km21) spg-7*(RNAi): 29/50	4c
wild-type control vs *mlk-1(ok2471)* control	0.0001	wild-type control: 38/50, *mlk-1(ok2471)* control: 28/50	4d
wild-type control vs wild-type *spg-7*(RNAi)	<0.0001	wild-type control: 38/50, vs wild-type *spg-7*(RNAi): 33/50	4d
mlk-1(ok2471) control vs *mlk-1(ok2471) spg-7*(RNAi)	<0.0001	*mlk-1(ok2471)* control: 28/50 vs *mlk-1(ok2471) spg-7*(RNAi): 49/50	4d
wild-type control vs wild-type *spg-7*(RNAi)	<0.0001	wild-type control: 50/50, wild-type *spg-7*(RNAi): 28/50	4e
wild-type *spg-7*(RNAi) vs *atfs-1(tm4919) spg-7*(RNAi)	<0.0001	wild-type *spg-7*(RNAi): 28/50 *atfs-1(tm4919) spg-7*(RNAi): 28/50	4e
wild-type spg-7(RNAi) vs *zip-2(4248)* spg-7(RNAi)	0.0004	wild-type spg-7(RNAi): 28/50, *zip-2(4248) spg-7*(RNAi): 39/50	4e
glp-4(bn2) control vs *glp-4(bn2) spg-7*(RNAi)	<0.0001	*glp-4(bn2)* control: 32/50, *glp-4(bn2) spg-7*(RNAi): 19/50	ED 5f
glb-4(bn2) spg-7(RNAi) vs *atfs-1(tm4919) spg-7*(RNAi)	<0.0001	*glb-4(bn2) spg-7*(RNAi): 19/50, *atfs-1(tm4919) spg-7*(RNAi): 32/50	ED 5f
wild-type control vs *atfs-1(et18)* control	0.0001	wild-type control: 40/50, *atfs-1(et18)* control: 35/50	ED 6f
wild-type control vs wild-type *lys-2*(RNAi)	0.0419	wild-type control: 40/50, *lys-2*(RNAi): 38/50	ED 6f
atfs-1(et18) control vs *atfs-1(et18) lys-2*(RNAi)	0.0004	*atfs-1(et18)* control: 35/50, *atfs-1(et18) lys-2*(RNAi): 44/50	ED 6f
wild-type control vs *atfs-1(et18) lys-2*(RNAi)	0.7317	wild-type control: 40/50, *atfs-1(et18) lys-2*(RNAi): 44/50	ED 6f
wild-type control vs wild-type *atp-2*	<0.0001	wild-type control: 36/50, wild-type *atp-2:* 31/50	ED 7c
wild-type control vs wild-type *eft-2*	<0.0001	wild-type control: 36/50, wild-type *eft-2:* 50/50	ED 7c
wild-type control vs wild-type *sca-1*	<0.0001	wild-type control: 36/50, wild-type *sca-1:* 34/50	ED 7c

Author Manuscript Author Manuscript Author Manuscript Author Manuscript

Strain comparison	*p* values	Number of worms	Figure
wild-type control vs wild-type *T25B9.9*	<0.0001	wild-type control vs wild-type *T25B9.9:* 50/50	ED 7c
wild-type control vs wild-type *T08A11.2*	0.1536	wild-type control vs wild-type *T08A11.2:* 37/50	ED 7c
wild-type control vs wild-type *atp-2*	<0.0001	wild-type control: 37/50, wild-type *atp-2:* 31/50	ED 7d
wild-type control vs wild-type *spg-7*(RNAi)	<0.0001	wild-type control: 37/50, wild-type *spg-7*(RNAi): 38/50	ED 7d
wild-type control vs wild-type *eft-2*	0.6435	wild-type control: 37/50, wild-type *eft-2:* 28/50	ED 7d
wild-type control vs wild-type *sca-1*	<0.0001	wild-type control: 37/50, wild-type *sca-1:* 48/50	ED 7d
wild-type control vs wild-type *T25B9.9*	0.2626	wild-type control: 37/50, wild-type *T25B9.9:* 38/50	ED 7d
wild-type control vs wild-type *T08A11.2*	<0.0001	wild-type control: 37/50, wild-type *T08A11.2:* 43/50	ED 7d

ED= Extended Data

Supplementary Material

Refer to Web version on PubMed Central for supplementary material.

ACKNOWLEDGMENTS

We thank Emily Troemel, Marc Pilon, Shohei Mitani of the National Bioresource Project, and the Caenorhabditis Genetics Center for providing *C. elegans* strains. We thank Dennis Kim and Joao Xavier for providing *P. aeruginosa* strains, and Thomas Langer and Simon Troeder for mammalian reagents. This work was supported by the Ellison Medical Foundation, the Lucille Castori Center for Microbes, Inflammation and Cancer at MSKCC and the National Institutes of Health (R01AG040061) to CMH, (F32AI100501) to NVK and (R01AI085581) to F. Ausubel.

REFERENCES

1. Melo JA, Ruvkun G. Inactivation of conserved C. elegans genes engages pathogen- and xenobiotic-associated defenses. Cell. 2012; 149:452–466. [PubMed: 22500807]
2. McEwan DL, Kirienko NV, Ausubel FM. Host translational inhibition by Pseudomonas aeruginosa Exotoxin A Triggers an immune response in Caenorhabditis elegans. Cell Host Microbe. 2012; 11:364–374. [PubMed: 22520464]
3. Dunbar TL, Yan Z, Balla KM, Smelkinson MG, Troemel ER. C. elegans detects pathogen-induced translational inhibition to activate immune signaling. Cell Host Microbe. 2012; 11:375–386. [PubMed: 22520465]
4. Wright G, Terada K, Yano M, Sergeev I, Mori M. Oxidative stress inhibits the mitochondrial import of preproteins and leads to their degradation. Exp Cell Res. 2001; 263:107–117. [PubMed: 11161710]
5. Nargund AM, Pellegrino MW, Fiorese CJ, Baker BM, Haynes CM. Mitochondrial import efficiency of ATFS-1 regulates mitochondrial UPR activation. Science. 2012; 337:587–590. [PubMed: 22700657]
6. Kim DH, et al. A conserved p38 MAP kinase pathway in Caenorhabditis elegans innate immunity. Science. 2002; 297:623–626. [PubMed: 12142542]
7. Twumasi-Boateng K, et al. An age-dependent reversal in the protective capacities of JNK signaling shortens Caenorhabditis elegans lifespan. Aging Cell. 2012; 11:659–667. [PubMed: 22554143]
8. Guarner F, Malagelada JR. Gut flora in health and disease. Lancet. 2003; 361:512–519. [PubMed: 12583961]
9. Newton K, Dixit VM. Signaling in innate immunity and inflammation. Cold Spring Harb Perspect Biol. 2012; 4

Author Manuscript Author Manuscript Author Manuscript Author Manuscript

10. Troemel ER, et al. p38 MAPK regulates expression of immune response genes and contributes to longevity in C. elegans. PLoS Genet. 2006; 2:e183. [PubMed: 17096597]
11. Kato Y, et al. abf-1 and abf-2, ASABF-type antimicrobial peptide genes in Caenorhabditis elegans. Biochem J. 2002; 361:221–230. [PubMed: 11772394]
12. Nandakumar M, Tan MW. Gamma-linolenic and stearidonic acids are required for basal immunity in Caenorhabditis elegans through their effects on p38 MAP kinase activity. PLoS Genet. 2008; 4:e1000273. [PubMed: 19023415]
13. Nicholas HR, Hodgkin J. Responses to infection and possible recognition strategies in the innate immune system of Caenorhabditis elegans. Mol Immunol. 2004; 41:479–493. [PubMed: 15183927]
14. De Smet K, Contreras R. Human antimicrobial peptides: defensins, cathelicidins and histatins. Biotechnol Lett. 2005; 27:1337–1347. [PubMed: 16215847]
15. O'Malley YQ, et al. Subcellular localization of Pseudomonas pyocyanin cytotoxicity in human lung epithelial cells. Am J Physiol Lung Cell Mol Physiol. 2003; 284:L420–L430. [PubMed: 12414438]
16. Gallagher LA, Manoil C. Pseudomonas aeruginosa PAO1 kills Caenorhabditis elegans by cyanide poisoning. J Bacteriol. 2001; 183:6207–6214. [PubMed: 11591663]
17. Estes KA, Dunbar TL, Powell JR, Ausubel FM, Troemel ER. bZIP transcription factor zip-2 mediates an early response to Pseudomonas aeruginosa infection in Caenorhabditis elegans. Proc Natl Acad Sci U S A. 2010; 107:2153–2158. [PubMed: 20133860]
18. Pukkila-Worley R, et al. Stimulation of host immune defenses by a small molecule protects C. elegans from bacterial infection. PLoS Genet. 2012; 8:e1002733. [PubMed: 22719261]
19. Tan MW, Mahajan-Miklos S, Ausubel FM. Killing of Caenorhabditis elegans by Pseudomonas aeruginosa used to model mammalian bacterial pathogenesis. Proc Natl Acad Sci U S A. 1999; 96:715–720. [PubMed: 9892699]
20. Gomes LC, Di Benedetto G, Scorrano L. During autophagy mitochondria elongate, are spared from degradation and sustain cell viability. Nat Cell Biol. 2011; 13:589–598. [PubMed: 21478857]
21. Feng J, Bussiere F, Hekimi S. Mitochondrial electron transport is a key determinant of life span in Caenorhabditis elegans. Dev Cell. 2001; 1:633–644. [PubMed: 11709184]
22. Kirienko NV, et al. Pseudomonas aeruginosa disrupts Caenorhabditis elegans iron homeostasis, causing a hypoxic response and death. Cell Host Microbe. 2013; 13:406–416. [PubMed: 23601103]
23. Tan MW, Rahme LG, Sternberg JA, Tompkins RG, Ausubel FM. Pseudomonas aeruginosa killing of Caenorhabditis elegans used to identify P. aeruginosa virulence factors. Proc Natl Acad Sci U S A. 1999; 96:2408–2413. [PubMed: 10051655]
24. Richardson CE, Kooistra T, Kim DH. An essential role for XBP-1 in host protection against immune activation in C. elegans. Nature. 2010; 463:1092–1095. [PubMed: 20182512]
25. Baker BM, Nargund AM, Sun T, Haynes CM. Protective coupling of mitochondrial function and protein synthesis via the eIF2alpha kinase GCN-2. PLoS Genet. 2012; 8:e1002760. [PubMed: 22719267]
26. Walter L, Baruah A, Chang HW, Pace HM, Lee SS. The homeobox protein CEH-23 mediates prolonged longevity in response to impaired mitochondrial electron transport chain in C. elegans. PLoS Biol. 2011; 9:e1001084. [PubMed: 21713031]
27. Rauthan M, Ranji P, Aguilera Pradenas N, Pitot C, Pilon M. The mitochondrial unfolded protein response activator ATFS-1 protects cells from inhibition of the mevalonate pathway. Proc Natl Acad Sci U S A. 2013; 110:5981–5986. [PubMed: 23530189]
28. Kim DH, et al. Integration of Caenorhabditis elegans MAPK pathways mediating immunity and stress resistance by MEK-1 MAPK kinase and VHP-1 MAPK phosphatase. Proc Natl Acad Sci U S A. 2004; 101:10990–10994. [PubMed: 15256594]
29. Runkel ED, Liu S, Baumeister R, Schulze E. Surveillance-activated defenses block the ROS-induced mitochondrial unfolded protein response. PLoS Genet. 2013; 9:e1003346. [PubMed: 23516373]
30. Liu Y, Samuel BS, Breen PC, Ruvkun G. Caenorhabditis elegans pathways that surveil and defend mitochondria. Nature. 2014; 508:406–410. [PubMed: 24695221]

Author Manuscript Author Manuscript Author Manuscript Author Manuscript

METHODS REFERENCES

31. Yoneda T, et al. Compartment-specific perturbation of protein handling activates genes encoding mitochondrial chaperones. J Cell Sci. 2004; 117:4055–4066. [PubMed: 15280428]
32. Rual JF, et al. Toward improving Caenorhabditis elegans phenome mapping with an ORFeome-based RNAi library. Genome Res. 2004; 14:2162–2168. [PubMed: 15489339]
33. Ehses S, et al. Regulation of OPA1 processing and mitochondrial fusion by m-AAA protease isoenzymes and OMA1. J Cell Biol. 2009; 187:1023–1036. [PubMed: 20038678]
34. Zhao Q, et al. A mitochondrial specific stress response in mammalian cells. Embo J. 2002; 21:4411–4419. [PubMed: 12198143]
35. Tan MW, Mahajan-Miklos S, Ausubel FM. Killing of Caenorhabditis elegans by Pseudomonas aeruginosa used to model mammalian bacterial pathogenesis. Proc Natl Acad Sci U S A. 1999; 96:715–720. [PubMed: 9892699]
36. Liu Y, Samuel BS, Breen PC, Ruvkun G. Caenorhabditis elegans pathways that surveil and defend mitochondria. Nature. 2014; 508:406–410. [PubMed: 24695221]
37. Nargund AM, Pellegrino MW, Fiorese CJ, Baker BM, Haynes CM. Mitochondrial import efficiency of ATFS-1 regulates mitochondrial UPR activation. Science. 2012; 337:587–590. [PubMed: 22700657]
38. Kennedy S, Wang D, Ruvkun G. A conserved siRNA-degrading RNase negatively regulates RNA interference in C. elegans. Nature. 2004; 427:645–649. [PubMed: 14961122]
39. Benedetti C, Haynes CM, Yang Y, Harding HP, Ron D. Ubiquitin-like protein 5 positively regulates chaperone gene expression in the mitochondrial unfolded protein response. Genetics. 2006; 174:229–239. [PubMed: 16816413]
40. Kirienko NV, et al. Pseudomonas aeruginosa disrupts Caenorhabditis elegans iron homeostasis, causing a hypoxic response and death. Cell Host Microbe. 2013; 13:406–416. [PubMed: 23601103]

Author Manuscript Author Manuscript Author Manuscript Author Manuscript

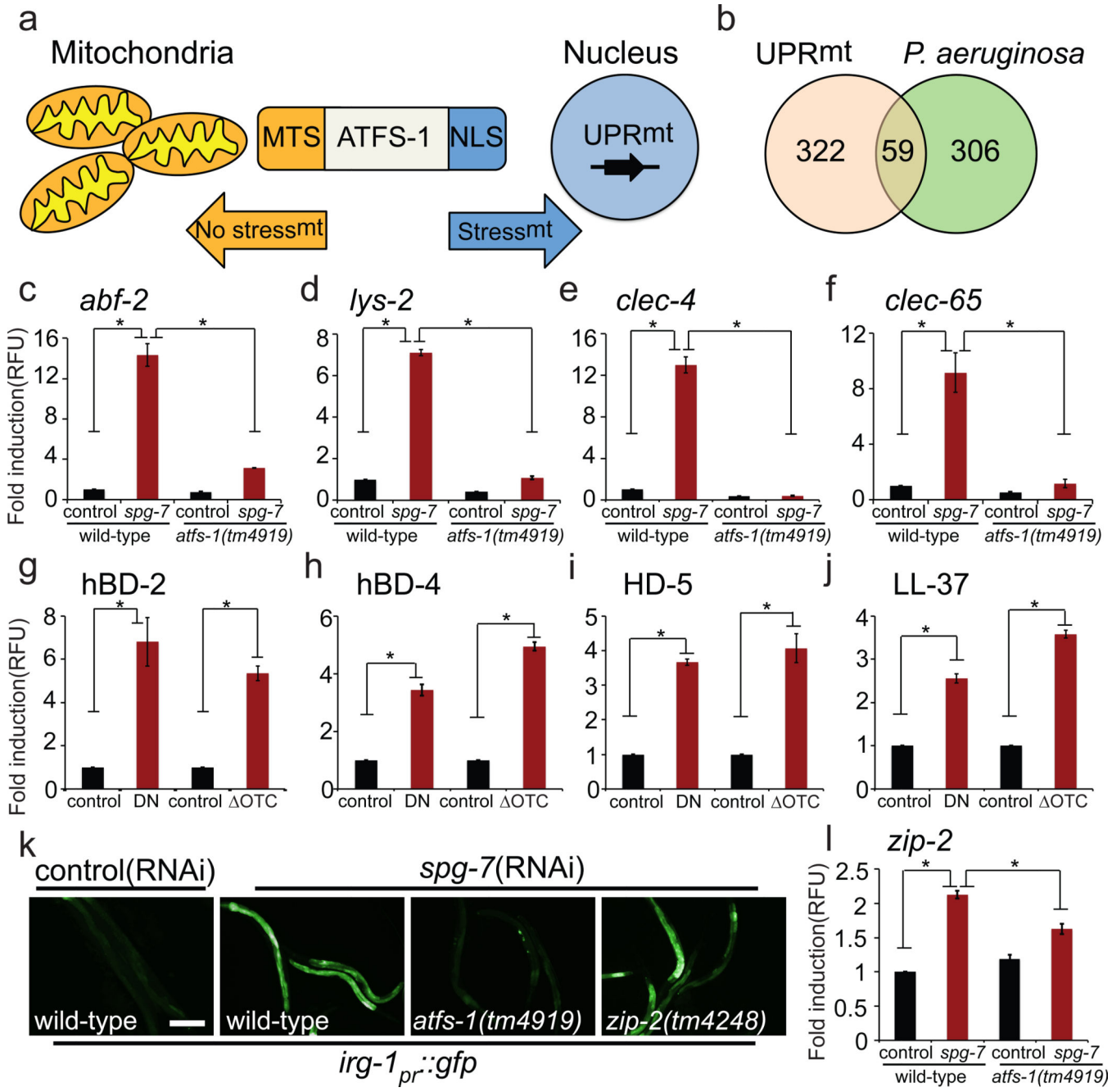

Figure 1. ATFS-1 induces innate immunity genes during mitochondrial dysfunction

a, UPR^{mt} regulation.

b, ATFS-1-dependent UPR^{mt} genes[5] in common with genes induced by *P. aeruginosa*[10].

c–f, *abf-2, lys-2, clec-4* and *clec-65* transcripts in wild-type or *atfs-1(tm4919)* worms on control versus *spg-7*(RNAi) (N=3, ± SD), * $p<0.05$ (Student's *t* test).

g–j, Antimicrobial peptide transcripts in mammalian cells during mitochondrial stress caused by expression of dominant-negative AFG3L2 (DN), or misfolded ornithine transcarbamylase (ΔOTC) (N=3, ± SD), * $p<0.05$ (Student's *t* test).

Author Manuscript Author Manuscript Author Manuscript Author Manuscript

k, *irg-1*$_{pr}$*::gfp* in wild-type, *atfs-1(tm4919)* or *zip-2(tm4248)* worms on control versus *spg-7*(RNAi). Scale bar, 0.15 mm.

l, *zip-2* transcripts in wild-type or *atfs-1(tm4919)* worms on control or *spg-7*(RNAi) (N=3, ± SD), * $p<0.05$ (Student's *t* test).

Author Manuscript Author Manuscript Author Manuscript Author Manuscript

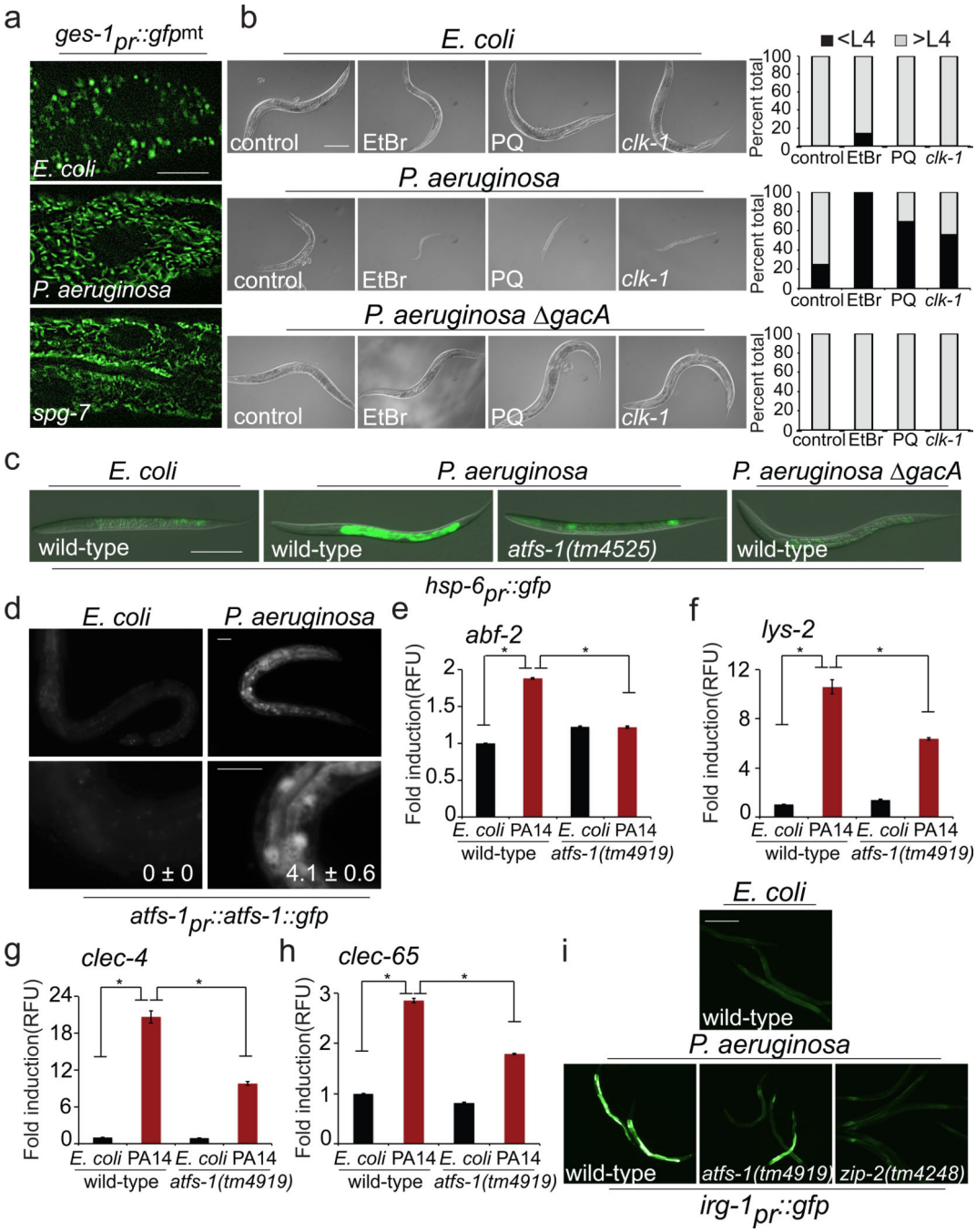

Figure 2. Mitochondrial stress and UPR^{mt} activation by *P. aeruginosa*

a, *ges-1*$_{pr}$*::gfp*^{mt} intestinal cell mitochondria on *E. coli*, *P. aeruginosa* or *spg-7*(RNAi). Scale bar, 0.05 mm.

b, Worms treated with ethidium bromide (EtBr), paraquat (PQ), and *clk-1(qm30)* worms raised on *E. coli*, *P. aeruginosa* or *P. aeruginosa* Δ*gacA*. Quantitation of the developmental stage for each treatment shown next to the corresponding panel (N=35 each treatment). Scale bar, 0.1 mm.

Author Manuscript Author Manuscript Author Manuscript Author Manuscript

c, Wild-type or *atfs-1(tm4525);hsp-6*$_{pr}$*::gfp* worms on *E. coli*, *P. aeruginosa* or *P. aeruginosa* Δ*gacA*. Scale bar, 0.1 mm.

d, *atfs-1*$_{pr}$*::atfs-1::gfp* on *E. coli* or *P. aeruginosa*. Lower panels are magnified. (N=3). Mean percentages of ATFS-1::GFP nuclear accumulation are indicated (± SEM). Scale bars, 0.1 mm.

e–h, *abf-2, lys-2, clec-4* and *clec-65* transcripts in wild-type or *atfs-1(tm4919)* worms on *E. coli* or *P. aeruginosa* (N=3, ± SD), * $p<0.05$ (Student's *t* test).

i, Wild-type, *atfs-1(tm4919)* and *zip-2(tm4248) irg-1*$_{pr}$*::gfp* worms on *E. coli* or *P. aeruginosa*. Scale bar, 0.05 mm.

Author Manuscript Author Manuscript Author Manuscript Author Manuscript

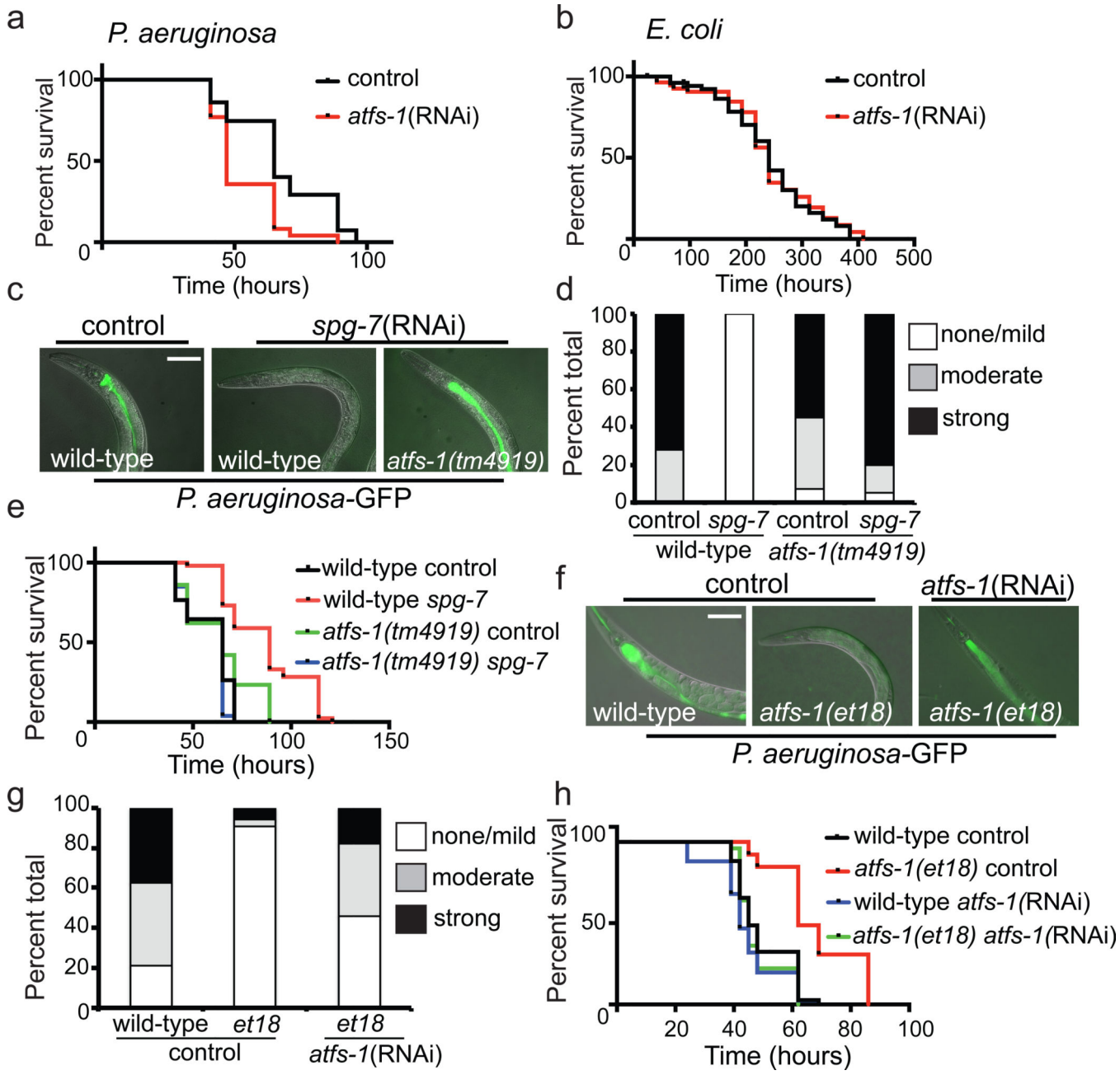

Figure 3. UPR^{mt} activation provides resistance to *P. aeruginosa*

a–b, Survival of worms on control or *atfs-1*(RNAi) exposed to *P. aeruginosa* or *E. coli*. Statistics are in Extended Data Table 3.

c–d, Images and quantitation of *P. aeruginosa*-GFP in wild-type or *atfs-1(tm4919)* worms on control or *spg-7*(RNAi). Scale bar, 0.1 mm. (N=35 each treatment).

e, Survival of wild-type and *atfs-1(tm4919)* worms on control or *spg-7*(RNAi) exposed to *P. aeruginosa*. Statistics are in Extended Data Table 3.

f–g, Images and quantitation of *P. aeruginosa*-GFP in wild-type and *atfs-1(et18)* worms on control or *atfs-1*(RNAi) (N=35 each treatment). Scale bar, 0.1 mm.

Author Manuscript Author Manuscript Author Manuscript Author Manuscript

h, Survival of wild-type and *atfs-1(et18)* worms on control or *atfs-1*(RNAi) exposed to *P. aeruginosa*. Statistics are in Extended Data Table 3.

Author Manuscript Author Manuscript Author Manuscript Author Manuscript

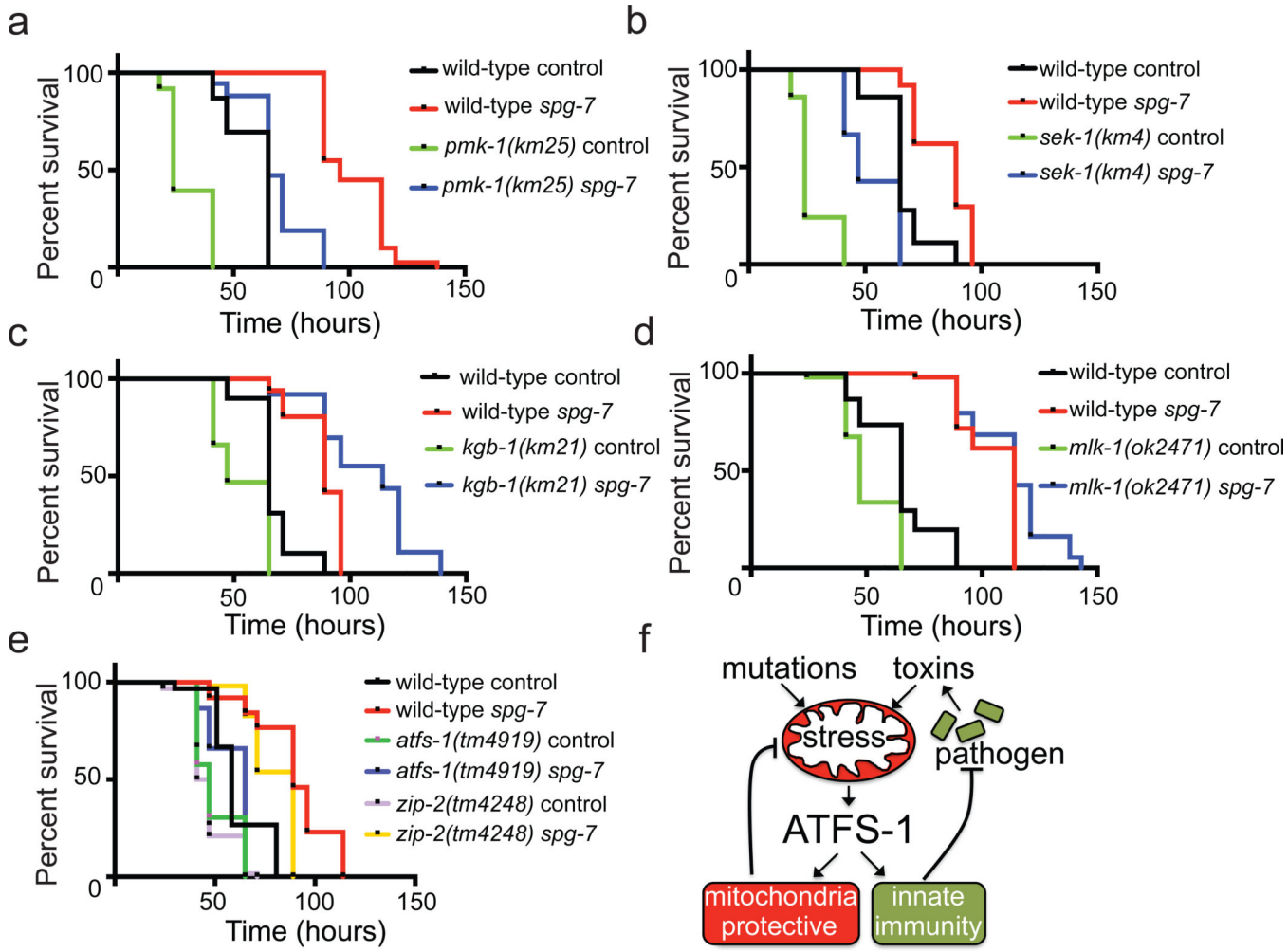

Figure 4. UPR^{mt} activation prolongs survival independent of known innate immune pathways

a–d, Survival of wild-type, *pmk-1(km25)*, *sek-1(km4)*, *kgb-1(km21)* and *mlk-1(ok2471)* worms on control or *spg-7*(RNAi) exposed to *P. aeruginosa*. Statistics are in Extended Data Table 3.

e, Survival of wild-type, *zip-2(tm4248)* and *atfs-1(tm4919)* worms raised on control or *spg-7*(RNAi) and exposed to *P. aeruginosa*. Statistics are in Extended Data Table 3.

f, ATFS-1 signaling schematic.